AGU PUBLICATIONS

JGR

Journal of Geophysical Research: Oceans

RESEARCH ARTICLE

10.1002/2015JC011204

Do deep-ocean kinetic energy spectra represent deterministic or stochastic signals?

Hans van Haren[1]

[1]Royal Netherlands Institute for Sea Research (NIOZ), Den Burg, The Netherlands

Key Points:
- Analyze ocean kinetic energy spectra as deterministic signals
- Nonlinear interaction between internal wave band and sub-inertial motions
- Spectral background outside peaks may be used for climatology studies on background variations

Correspondence to:
H. van Haren,
hans.van.haren@nioz.nl

Citation:
van Haren, H. (2016), Do deep-ocean kinetic energy spectra represent deterministic or stochastic signals?, *J. Geophys. Res. Oceans*, *121*, 240–251, doi:10.1002/2015JC011204.

Received 5 AUG 2015
Accepted 7 DEC 2015
Accepted article online 13 DEC 2015
Published online 10 JAN 2016

Abstract In analogy with historic analyses of shallow-water tide-gauge records, in which tides and their higher harmonics are modified by sea level changes induced by atmospheric disturbances, it is shown that deep-sea currents can be interpreted as motions at predominantly inertial-tidal harmonic frequencies modified by slowly varying background conditions. In this interpretation, their kinetic energy spectra may not be smoothed into a quasi-stochastic continuum for (random-)statistic confidence. Instead, they are considered as quasi-deterministic line-spectra. Thus, the climatology of the internal wave field and its slowly varying background can be inferred from line spectra filling the cusps around nonlinear tidal-inertial harmonics, as suggested previously.

1. Introduction

Sea level ("tide") gauges in ports and shallow seas are amongst the oldest oceanographic instruments. As a result, their records provide virtually uninterrupted oceanographic time series of many years long. Such records have been studied predominantly for tidal harmonics, since Lord Kelvin, G. Darwin and A. Doodson about a century ago. As barotropic surface tides are considered purely deterministic signals with well-defined amplitudes and phases, tide-gauge records are thought to provide unbiased estimates of different harmonics. Depending on the length of the time series, a large number of tidal harmonics can be distinguished. This large number was partially due to subtle variations of the earth-moon-sun system, such as the 8.8 y lunar perigee and the 18.6 y nodal modulations, resulting in extra components in addition to the main lunar and solar constituents in the expansion of the tidal potential. Nonlinear interactions, predominantly in shallow seas responding to astronomical forcing, also cause overtides (higher harmonics) of the main constituents [e.g., *Rossiter and Lennon*, 1968; hereinafter RL].

However, despite the deterministic character of the tidal potential, recorded signals do not appear as purely deterministic, as their spectra show no gaps between spectral lines [*Munk et al*., 1965; *Munk and Cartwright*, 1966]. Partially, this is due to the influence of unresolved neighboring constituents, when these are not separated by a fundamental bandwidth related to the finite length of the record. This modulation also results in a change in variance at the principle harmonic frequencies; it is captured via the f,u factors in harmonic analysis or, alternatively, via the admittance function proposed by *Munk and Cartwright* [1966]. In addition, this has been attributed to deterministic signals being embedded in stochastic signals sometimes called "noise" induced by instrumental nonlinear response or, more important, by variable environmental effects, such as atmospheric disturbances causing unpredictable sea level changes in shallow seas [*Munk and Cartwright*, 1966].

Following common practice, the statistical treatment of the embedding in stochastic signals aims to reduce variance at the expense of the spectral resolution and biased spectral estimates of the deterministic signals [*Jenkins and Watts*, 1968]. In general however, tide gauge records are not treated statistically, and broadening of line spectra ("periodograms") is considered due to "quasi-deterministic" nonlinear interactions between tidal constituents and atmospheric disturbances, resulting in "tidal cusps" [*Munk et al*., 1965]. RL assigned many spectral lines to nonlinear tidal-tidal interactions, which are embedded in a non-zero spectral continuum due to tidal interaction frequencies and their atmospherically induced broadening.

In contrast with tide gauge records, open ocean current meter records have been often considered stochastic [e.g., *Garrett and Munk*, 1972; hereinafter GM] rather than deterministic, except perhaps for tidal analysis (e.g., *Munk et al*. [1970] for near-bottom records and *Wunsch* [1975] for open-ocean records). This resulted in

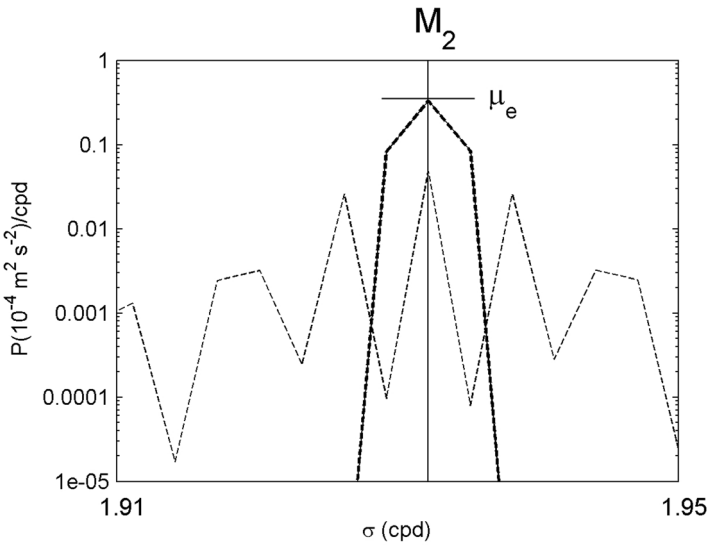

Figure 1. "Line-spectrum" appearance of an artificial model of a single harmonic signal (at $\sigma = M_2$, the principle lunar semi-diurnal) after its record of length T = 333 d was tapered with a single Kaiser-Bessel window prior to Fourier transform (thin solid line peak). The effective fundamental bandwidth ($\mu_e = 2.2/T$) is indicated by the horizontal bar. Note the large drop-off in variance by more than 4 orders of magnitude at $\sigma = M_2 \pm 0.6\mu_e$. To resolve the deterministic signal indicated by the thin vertical line one would need a record of 20 y in length. The thick dashed spectrum is for the same single harmonic time series but mimicking a mechanical current meter stalling 10% of the time. The thin dashed spectrum is for the same single harmonic time series but modeling an interaction of the tidal harmonic with a sub-inertial current by having zero amplitude over two data portions of (arbitrary) 84 days, about 20% of the record (for details, see *van Haren* [2004a]).

a general spectral slope of the "internal wave band" fit to West-Atlantic and Mediterranean data with weak tides in order to obtain a consistent kinematic model of one of ocean's most energetic motions. The GM-model does not include tidal harmonics and other nonlinearly modified motions. Thus, at the expense of spectral resolution, band averaging is applied to long current meter records to enhance the number of degrees of freedom (ν [df]) for improved statistics on spectral estimates by reduction of "noise" (for the method, see e.g., *Emery and Thomson* [1998]). The statistical significance commonly applied to kinetic energy spectra uses the chi-squared distribution [e.g., *Jenkins and Watts*, 1968], which rapidly tends to a normally distributed signal for increasing ν.

The above difference in treatment of spectra from tide gauge and current meter records was for good reason, because current meters are considered to sample more undetermined signals, for example due to nonlinear instrumental response, mooring motions, and because linear surface tidal signals are considered less dominant in the open ocean. However, *van Haren* [2004a] showed that the background spectral level in the semi-diurnal tidal band of yearlong current meter records around 4000 m in the Bay of Biscay is mainly attributable to interactions between tidal and low-frequency (sub-inertial) currents, similar to the cusps in shallow sea tide gauge records. Using simple models, the effects of imperfect moored (mechanical) current meters has been shown to be minimal and at least one order of magnitude smaller than the observed "continuum." As the same sub-inertial background motions also interact with near-inertial motions, which are not registered in tide (here pressure) gauge records, the bandwidths of near-inertial and semi-diurnal tidal motions have been observed to be about equal [*van Haren*, 2004b]. It appeared that a GM spectral roll-off rate can be obtained even from a spiked deterministic record including nonlinear higher harmonics from the NE-Atlantic upon heavy smoothing so that the internal wave band appears as a continuum [*van Haren et al.*, 2002].

As motions at inertial and tidal frequencies dominate the variance of deep-ocean kinetic energy spectra and as they are the main sources of internal waves [e.g., *LeBlond and Mysak*, 1978], the above current meter observations raised the question of the relative importance of deterministic and stochastic signals, in particular in the internal (inertio-gravity) wave frequency (σ) band $f \sim< \sigma \sim< N$, where f denotes the local inertial frequency and N the buoyancy frequency. To this one can add that the internal wave band continuum as presented in GM has a non-zero slope, making it distinctly different from white noise that has slope zero on a log-log scale, red −1-slope noise and blue noise. For typical ocean spectra the terminology "noise" is thus not entirely appropriate, or, as a reviewer stated "one man's noise is another man's signal."

In the present paper, I elaborate and aim to somewhat better understand the broadening of spectral lines in ocean current spectra, specifically for the energetic internal wave band, and its relation with the "continuous background spectrum." The understanding of deterministic versus stochastic signals may provide support for future studies on sources of the entire ocean continuum spectrum, and variations therein. The focus is on deep-sea current spectra far from the surface, in which wind-effects only play an indirect role.

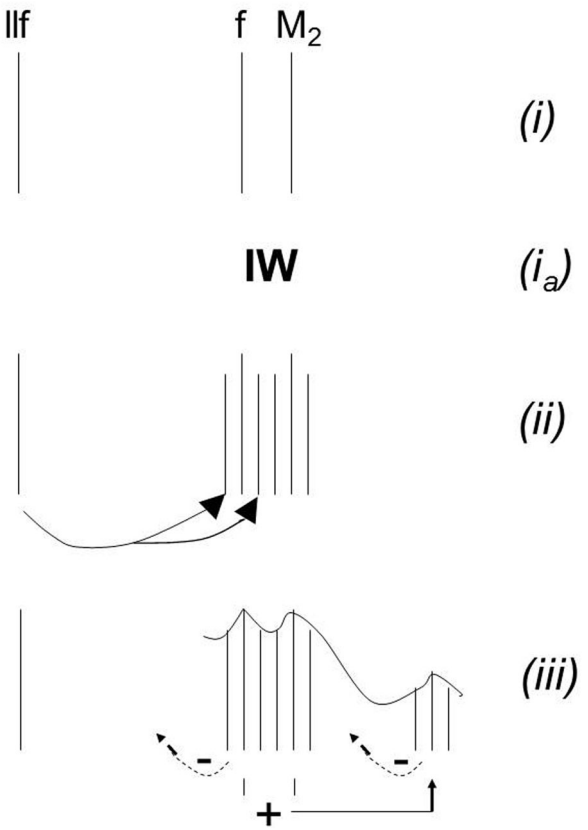

Figure 2. Impression of the filling of an ocean kinetic energy spectrum, following the steps below. (i) Motions are generated (externally) at only three distinguished (∼deterministic) frequencies: a tidal (M_2), inertial (f) and a low-frequency sub-inertial (llf). (ii) After energy transfer to internal waves (IW) at stage (i_a), nonlinear interactions with the low-frequency current result in a split of the tidal-inertial lines. Further splits following interaction between the same low-frequency current with the initial split lines create a quasi-continuum tidal-inertial band. (iii) Finally, the motions in these bands interact and fill the rest of the spectrum. This (re)generates some of the low-frequency motions, through (tidal) rectification, indicated by the -signs.

Table 1. Current Meter Mooring Details[a]

Mooring	BB8	BB3	FS
Latitude (N)	45°48′	46°39′	60°58′
Longitude (W)	06°50′	05°29′	03°15′
Waterdepth (m)	4810	2450	850
f (cpd)	1.437	1.458	1.752
Current meter type	RCM8	RCM8	ADCP
Instrument depth (m)	3810	1450	843 (data:750)
N (cpd)	7–10	23–35	70–110
Sampling period	Jul 1995 to Jun 1996	Jul 1995 to June 1996	May–Oct 1999
Sampling interval (min)	20	20	10
Typical speed (m s^{-1})	0.08	0.15	0.3
Maximum speed (m s^{-1})	0.12	0.25	0.75

[a]BB denotes Bay of Biscay, FS Faroe-Shetland Channel, 1 cpd = $2\pi/86400$ s^{-1}, f denotes the local inertial frequency and N the buoyancy frequency over 100 m vertical scales. RCM8 indicates mechanical Aanderaa single point current meter; ADCP a 75 kHz TeleDyne/RDI Long-Ranger acoustic Doppler current profiler.

These effects are mainly communicated through inertial motions, sub-inertial large-scale (boundary) currents and slowly varying background stratification variations.

2. Spectral Analysis of Deterministic and Stochastic Signals

In their powerful treatise on spectral analysis, *Jenkins and Watts* [1968] stress the difference between deterministic and stochastic signals. The Fourier decomposition of the former is well defined, so that longer time series yield more estimates of amplitude (and phase) at a particular frequency and converge to the "true" values, simply because the fundamental frequency band becomes smaller. In order to obtain meaningful quantitative information from the spectrum of a stochastic signal, several periodogram estimates are averaged, resulting in a "smoothed" spectrum. The associated chi-squared distribution of statistical significance is thus applicable for a near-Gaussian stochastic process, but has not much relevance for a pure deterministic process. The question is, what process an open-ocean current time series best represents.

In the spectral analysis applied here, different levels of smoothing are used for comparison. A "raw" spectrum is defined as the spectrum for $\nu \approx 3$ df, which is obtained after multiplying the time series with a single Kaiser-Bessel (modified cosine-bell shaped) [*Parks and Burrus*, 1987] window over the entire record. After application of this window, side-band ripples are reduced by several orders of magnitude (Figure 1) at the expense of a slightly increased fundamental bandwidth: the effective fundamental bandwidth $\mu_e \approx 2.2/T$, T denoting the length of time series, at the level of one decade (order of magnitude) below the peak value. In the figures below, in which weak smoothing is applied, no confidence levels of statistical significance are given (95% confidence interval would extend ∼1.5 decades in the vertical), because most individual peaks are not significant from the viewpoint of random statistics. Further smoothing is obtained by averaging spectral estimates of smaller parts, of length M data points, of the total record of N data points. Each smaller portion is half-overlapping its neighbors and is tapered by the same approximate cosine-bell

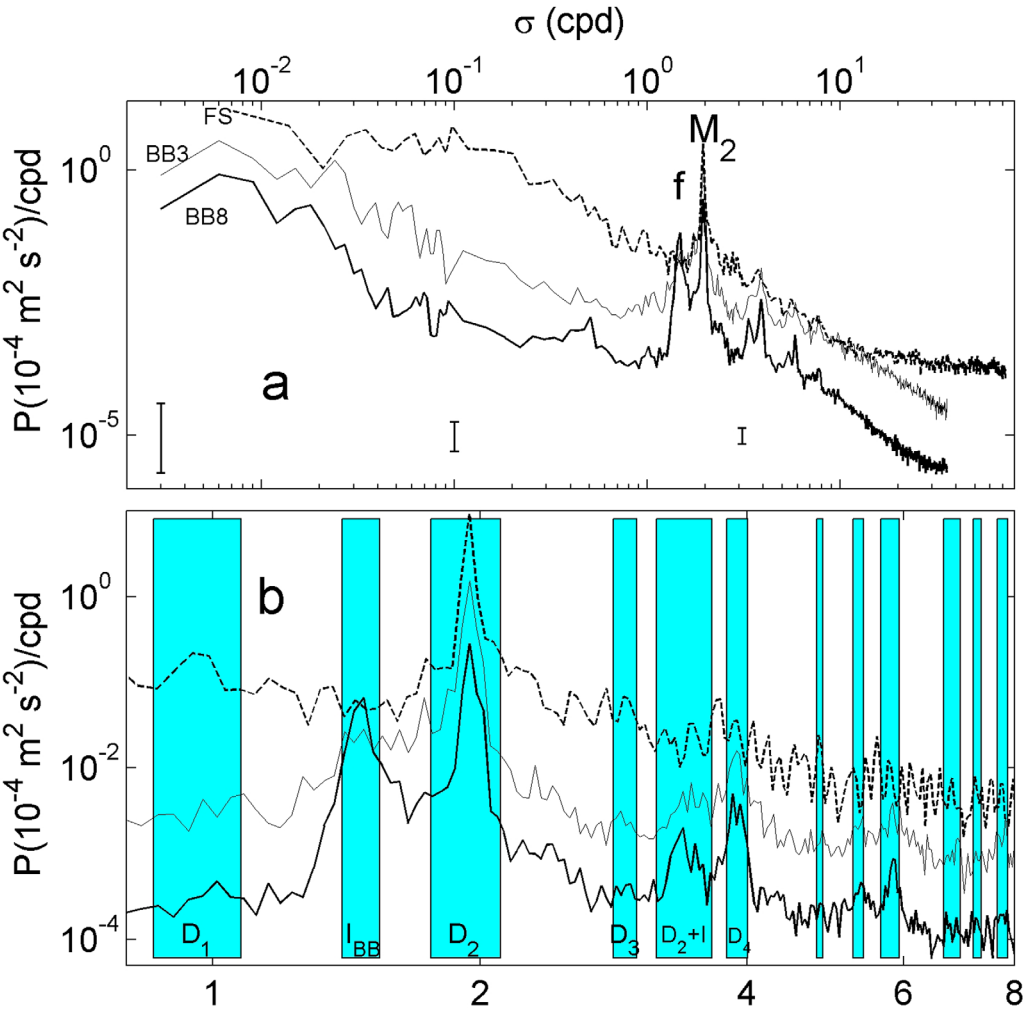

Figure 3. (a) Kinetic energy spectra, frequency-dependently smoothed for clarity, from: 11 months of current meter observations at $z = -3810$ m on mooring BB8 in the Bay of Biscay (lowest graph) and $z = -1450$ m at BB3 (middle graph; thin), 5 months of ADCP observations in the Faeroe-Shetland Channel at $z = -750$ m (FS; upper graph). The spectra are not offset vertically. As shown by the three vertical bars indicating the 95% confidence interval using random statistics, smoothing varies from nearly unsmoothed ($\nu \approx 3$ df; degrees of freedom) for $\sigma < 0.1$ cpd, moderately smoothed ($\nu \approx 10$ df) for $0.1 < \sigma < 3$ cpd, and relatively heavily smoothed ($\nu \approx 50$ df) for $\sigma > 3$ cpd. (b) Detail of Figure 3a, with FS off-set vertically by a factor of 3 for clarity. Shading indicates various frequency bands, from left to right: the diurnal band, inertial (applicable for BB data only), semi-diurnal (includes FS inertial), ter-diurnal, inertial-semi-diurnal, quarter-diurnal, fifth-diurnal, inertial-quarter-diurnal, sixth-diurnal, seventh-diurnal, inertial-sixth-diurnal and eighth-diurnal.

shaped window, so that $\nu \approx$ (3.8N/M - 3.2)df [*Nuttall and Carter*, 1980]. As bispectra, for studying resonant nonlinear interactions [*Kim and Powers*, 1979], require considerable smoothing for statistical significance using ocean data [*McComas and Briscoe*, 1980; *Carter and Gregg*, 2006], they are not useful for the present study.

As a conceptual model we adopt, in analogy with tidal spectroscopy line-splitting due to slow modulation of tides by deterministic long-term variations like lunar nodal [e.g., *Munk and Cartwright*,1966], the viewpoint of a transfer of energy from, initially, three sources at different frequencies: quasi-deterministic tidal, inertial and an, unspecified, large-scale low-frequency sub-inertial (Figure 2i). The nonlinear interaction as in advection between the latter and the former two will create side-bands following a split of energy away from the main spectral lines (Figure 2ii). Multiple interactions will create finite bandwidths or cusps. Nonlinear interactions between the motions within the cusps will generate cusps around higher harmonics, as in *van Haren et al*. [2002]. Eventually, the entire spectral continuum may be filled (Figure 2iii). The filling can include forward (sum-frequency interactions) and backward (difference-frequency interactions) energy transfer. Here, we attempt to retrace the decomposition of the continuum into spectral lines from current meter observations.

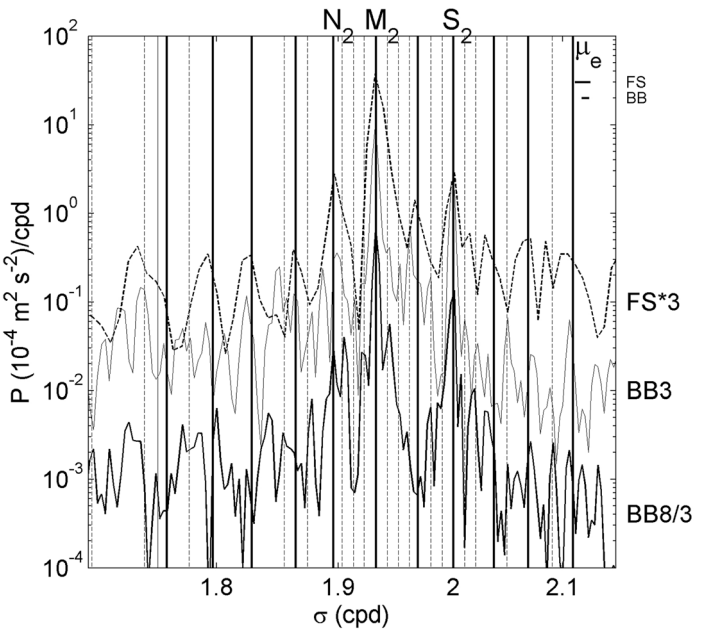

Figure 4. Unsmoothed ($\nu \approx 3$ df) detail of Figure 3a with BB8 off-set vertically by a factor of 1/3 and FS by a factor of 3: the semi-diurnal band. Vertical lines indicate the frequencies in Table 2, with the RL-lines [*Rossiter and Lennon*, 1968] indicated by thick solid lines, the *-indicated frequencies by thin solid lines and the $^{\&}$-indicated frequencies by thin dashed lines. The fundamental bandwidths of $\mu_e = 0.007$ cpd for BB data, and $\mu_e = 0.015$ cpd for FS data are indicated by horizontal bars in the top right.

Table 2. Astronomical and Compound Frequencies up to the Eighth-Diurnal Band After, After (Rossiter and Lennon, 1968; RL).[a]

Name	Origin	σ(cpd)
Diurnal		
$2Q_1$		0.8569
$^{\&}0.97M_2$-S_1		0.8743
Q_1		0.8932
$^{\&}0.99M_2$-S_1		0.9129
O_1		0.9295
$^{\&}0.97M_1$		0.9371
$^{\&}0.98M_1 \sim N_1$		0.9468
$^{\&}0.995M_1$		0.9613
M_1		0.9661
$^{\&}1.005M_1$		0.9719
$^{\&}1.02M_1 \sim M_2 - N_1$		0.9855
$^{\&}1.03M_1$		0.9951
K_1		1.0027
$^{\&}S_2 - 1.005M_1$		1.0290
J_1		1.0390
$^{\&}S_2 - 0.99M_1$		1.0435
SO_1		1.0705
Inertial (latitude: $\varphi = 45.800°$; BB8)		
*0.96f		1.3800
*0.97f		1.3944
*0.98f		1.4088
*0.99f		1.4232
*f		1.4376
*1.005f		1.4447
*1.01f		1.4519
$*^{\&}f(\varphi = 46.665°$;BB3)		1.4585
*1.015f		1.4591
*1.021f		1.4677
*1.03f		1.4807
*1.04f		1.4951
*1.08f		1.5526
*1.16f		1.6676

3. Data

Examples of moored (Eulerian) current observations are studied from the continental slope and near its foot in the abyssal plain of the Bay of Biscay (BB) and from the more energetic Faeroe-Shetland Channel (FS), both in the tidally dominated NE-Atlantic Ocean, see Table 1 for mooring details. At these mid- and high-latitude locations all dominant tidal harmonics were found within the frequency band of freely propagating internal gravity waves, except for (less energetic) diurnal constituents. The 5 and 11 months lengths of time series assured reasonable resolution of tidal and inertial bands, but did not resolve particular modulation evidence in these bands due to, e.g., lunar perigee and nodal variations.

In comparison with the mechanical current meter of the BB-moorings, the acoustic Doppler current profiler (ADCP) of the FS-mooring showed relatively high noise levels (Figure 3), but it did not suffer from instrumental errors during weak flows. Several tests showed (internal wave band) spectra from RCM-8 data to be little affected by instrumental nonlinear response, even above the abyssal plain where currents were relatively close to the 0.02 m s^{-1} threshold velocity of an RCM-8 [*van Haren*, 2004a]. The records from the instruments at BB3 and BB8 used here showed less than 10% data points below threshold so that the spectra are not affected by this instrumental flaw (Figure 1). The thick-dashed spectrum from model current meter stalling 10% of the time is indistinguishable from the thin solid line spectrum for a perfect model current meter, except for a leveling off around 10^{-12} m^2 s^{-2} cpd^{-1} outside the window displayed. Mooring motions were relatively small, e.g., from using

Table 2. (continued)

Name	Origin	σ(cpd)
Semi-diurnal		
$^{\&}0.84M_2$		1.6231
$^{\&}0.985\ 2MN2S_2$		1.7026
$^{\&}0.99\ 2MN2S_2$		1.7429
*f(φ =60.970°;FS)		1.7536
$2MN2S_2$	$2M_2+N_2-2S_2$	1.7605
$^{\&}1.01\ 2MN2S_2 \approx 0.92M_2$		1.7781
$3M2S_2$	$3M_2-2S_2$	1.7968
MNS_2		1.8283
$^{\&}0.96M_2$		1.8550
μ_2		1.8645
$^{\&}0.97M_2$		1.8743
N_2 (incl. ν_2)		1.8960
$^{\&}0.985M_2$		1.9033
$^{\&}0.99M_2$		1.9130
$^{\&}0.995M_2$		1.9223
M_2		1.9323
$^{\&}1.005M_2$		1.9420
$^{\&}1.01M_2$		1.9516
$^{\&}1.015M_2$		1.9613
L_2	$\sim 1.02M_2$	1.9686
$^{\&}0.99S_2$		1.9800
$^{\&}0.995S_2$		1.9900
S_2		2.0000
$^{\&}1.005S_2$		2.0100
$^{\&}1.01S_2$		2.0200
MSN_2		2.0363
$^{\&}2(0.992MN2S_2)$-f		2.0483
$2SM_2$		2.0678
$^{\&}2(1.012MN2S_2)$-f		2.0900
SKN_2	$S_2+K_2-N_2$	2.1095
Quarter-diurnal-sub-inertial		
*M_4-f(φ =60.970°;FS)		2.1110
*M_4-f(BB8)		2.4270
*$1.01M_4$-f(BB8)		2.4657
*MS_4-f(BB8)		2.4947
*S_4-f(BB8)		2.5624
Ter-diurnal		
MQ_3	M_2+Q_1	2.8255
MO_3		2.8618
*2f		2.8751
M_3		2.8984
$^{\&}0.99MK_3$	$0.99M_2+K_1$	2.9157
MK_3		2.9350
$^{\&}1.01MK_3$	$1.01M_2+K_1$	2.9543
$2MQ_3$	$2M_2-Q_1$	2.9713
SK_3		3.0027
Inertial(BB8)-semi-diurnal		
$^{\&*}0.98f+2MN2S_2$		3.1693
*f+$2MN2S_2$		3.1981
$^{\&*}f+2*0.99M_2-S_2$		3.2634
$^{\&*}f+(1.005+1)M_2-S_2$		3.3118
*f+N_2		3.3335
$^{\&*}f+1.01N_2$		3.3479
*f(BB3)+N_2	$\sim^{\&*}f+0.99M_2$	3.3545
*f+M_2		3.3698
$^{\&*}f+1.01M_2$		3.3892
*f(BB3)+M_2		3.3908
$^{*\&}1.021f+M_2$		3.4000
*f+S_2		3.4376
$^{\&*}f-0.99M_2+2S_2$		3.5246
*f(FS)+M_2		3.6859
Quarter-diurnal		
$2\mu_2$		3.7291
$^{\&}0.99M_2$	$+MNS_2$	3.7412
$^{\&}0.97M_4$		3.7486
$^{\&}3N_2-0.99M_2$		3.7750
$^{\&}0.98M_4$		3.7873

elliptical buoyancy on the short FS-mooring. Further effects on data due to typical sampling strategies of "point measurement" RCM-8 and "spatial averaging" (across ~ 100 m in the horizontal) ADCP will be discussed below. The three examples were chosen, because of differing sub-inertial motions, varying from relatively narrow band (~0.006 cpd) at BB8 to broadband 0.005–0.1 cpd at FS (Figure 3).

4. Observed Spectra

At all three sites the largest spectral value (kinetic energy content) of the low-frequency motions, the sub-inertial "peak," is comparable with the local tidal peak height (Figure 3). We observe differently peaked inertial band and, when distinguishable, tidal-tidal (M_2, M_4...) and tidal-inertial (M_2+f, M_4+f, ...) harmonics in the internal wave band. Peaks at these frequencies are most pronounced at BB8 and they merge more or less with the smoothly sloping spectral "continuum background" in the FS data (showing the broadest sub-inertial band).

van Haren [2004a] has shown that tidal motions were mostly (~70% of total energy) of barotropic nature for BB8-data and "coherent baroclinic" for BB3-data. The latter implies that internal tidal motions near a continental slope source were persistent in amplitude and phase over 11 months. The remaining ~30% of the tidal energy was due to "incoherent" baroclinic motions, showing intermittency in the time domain, and consisting of peaks at non-tidal constituent frequencies such as $(1.000 \pm 0.005)M_2$. These peaks have energy levels comparable to that of tidal constituent N_2 (Figure 4 and Table 2). The BB-data show many of them, which are attributed to local nonlinear interaction between tides and the

Table 2. (continued)

Name	Origin	σ(cpd)
$3MS_4$	$3M_2-K_2$	3.7968
$^{\&}0.995MN_4$	$0.995M_2+N_2$	3.8186
MN_4		3.8283
$^{\&}0.99M_4$	$0.99M_2+M_2$	3.8452
$^{\&}0.995M_4$	$0.995M_2+M_2$	3.8549
M_4		3.8645
$^{\&}1.005M_4$	$1.005M_2+M_2$	3.8742
$^{\&}1.01M_4$	$1.01M_2+M_2$	3.8839
$^{\&}1.015M_4$	$1.015M_2+M_2$	3.8935
$3MN_4$	$3M_2-N_2$	3.9008
$^{\&}0.995MS_4$	$0.995M_2+S_2$	3.9207
MS_4		3.9323
$^{\&}1.005MS_4$	$1.005M_2+S_2$	3.9419
S_4		4.0000
Fifth-diurnal		
$3MK_5$	$3M_2-K_1$	4.7941
$*2f+M_2$		4.8074
M_5		4.8307
$2MO_5$	$3M_2-O_1$	4.8673
Inertial(BB8)-quarter-diurnal		
$*0.973f+N_4$		5.1907
$*f+N_4$		5.2295
$*f+M_4$		5.3021
$*f(BB3)+M_4$		5.3230
$*1.021f+M_4$		5.3323
$*f+MS_4$		5.3698
$*f+S_4$		5.4376
$*1.073f+S_4$		5.5425
Sixth-diurnal		
$2(MN)S_6$	$2M_2+2N_2-S_2$	5.6565
$3MNS_6$	$3M_2+N_2-S_2$	5.6928
$4MS_6$	$4M_2-S_2$	5.7291
$*4f$		5.7502
$2MN_6$		5.7605
M_6		5.7968
MSN_6		5.8283
$MK\nu_6$	$M_2+K_2+\nu_2$	5.8386
$2MS_6$		5.8645
$3MSN_6$	$3M_2+S_2-N_2$	5.9008
$2SM_6$		5.9323
Seventh-diurnal		
$*2f+M_4$		6.7397
M_7		6.7630
Inertial(BB8)-sixth-diurnal		
$*0.973f+N_6$		7.0867
$*f+N_6$		7.1255
$*5f$		7.1878
$*f+M_6$,$2f(FS)+1.023f(FS)+M_2$		7.2344
$*f(BB3)+M_6$		7.2553
$*1.023f+M_6$		7.2674
$*f+S_6$		7.4376
$*1.073f+S_6$		7.5425
Eighth-diurnal		
$2(MN)_8$	$2M_2+2N_2$	7.6565
$3MN_8$	$3M_2+N_2$	7.6928
M_8		7.7291
$2MSN_8$	$2M_2+S_2+N_2$	7.7605
$3MS_8$	$3M_2+S_2$	7.7968
$MSNK_8$	$M_2+S_2+N_2+K_2$	7.8337
$2(MS)_8$	$2M_2+2S_2$	7.8645

[a]In addition to RL-identified constituent frequencies, several (modified) inertial frequencies are identified in Figures 4–8 (marked with asterisks (*) here. Superscript ($^{\&}$) indicates examples of non-harmonic constituents introduced here. These constituents are hypothesized to be due to interactions between motions at tidal frequencies and slowly varying background motions (in the Table only at 0.01 cpd). From RL, constituents are retained that are resolved using 11 months records, with an effective fundamental bandwidth of $\mu_e \approx 0.006$ cpd (BB). Frequency σ is in cycles per day, 1 cpd $= 2\pi/86400\ s^{-1}$. Values given are for 20 y records, $\mu_e \approx 0.00014$ cpd.

relatively well-defined low-frequency motions $\sigma_{lf} = 0.01 \pm 0.005$ cpd. At BB8, such peaks are coherent across vertical distances of 400 m, between neighboring current meters [*van Haren*, 2004a]. Following suggestions by RL, the registration may also reflect changes in the environmental conditions, here due to remote variations in the background current and stratification predominantly at this low frequency. A simple model mimicking the effects of such variations on sinusoidal motions, by switching the latter on/off twice, is in Figure 1 (thin dashed spectrum). The peak at the central frequency is reduced for this model spectrum, and the background in the form of the first sidelobe is increased by up to a factor of 0.1 of the peak-value of the original single harmonic.

Such nonlinear interaction, for example through the advection by semi-diurnal and 0.01 cpd waves or eddies yielding peaks at $(1.000 \pm 0.005)M_2$, is observed in the BB-data to extend into the rest of the spectrum. After repeated interactions it creates peaks at $(1.000 \pm 0.01)M_2$, $(1.000 \pm 0.015)M_2$ and $(1.000 \pm 0.02)M_2$, etcetera. In Table 2 and Figure 4 the observed split of tidal lines is included (rather than broadening) for other known tidal constituents. This extends the list from RL. In contrast, in the FS-data tides can interact with low-frequency motions over a broader frequency range. In the ADCP-record this results in larger overall semi-diurnal cusp levels (albeit not larger relative to the M_2 peak height), and better shows tidal constituents like μ_2, L_2, that are not observed in the BB-data (Figure 4).

Some similar observations are made for the diurnal band ("D_1"; Figure 5). It is noted that in the present data in this band motions

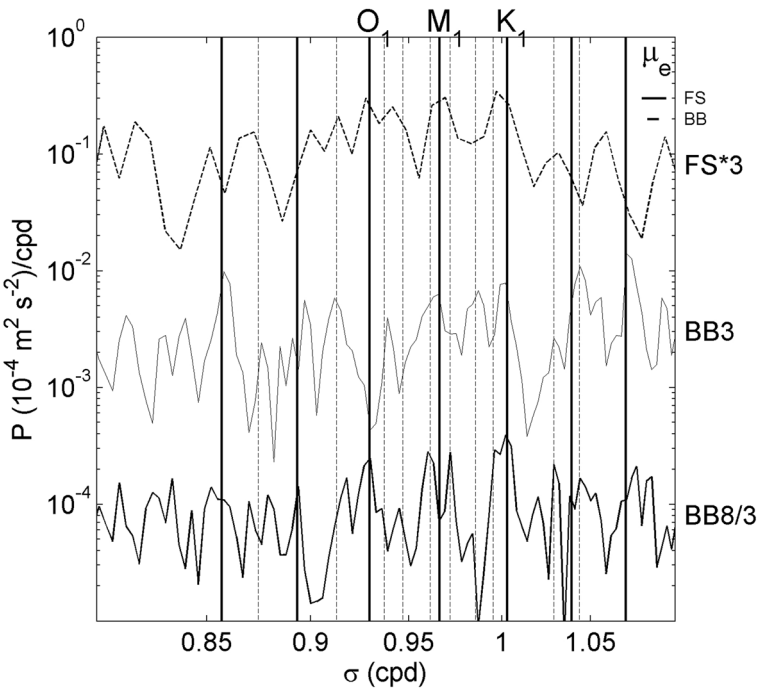

Figure 5. As Figure 4 but for the diurnal band.

at the tidal constituents (e.g., O_1, K_1) are not more energetic than at non-tidal frequencies: the tidal constituents are not significant in the common statistical sense. This is location and latitude dependent; here, diurnal frequencies are sub-inertial and motions outside the [f, N]-band cannot describe freely propagating internal waves. In the FS-data we observe M_1, the first sub-harmonic of the semi-diurnal lunar tide, while a

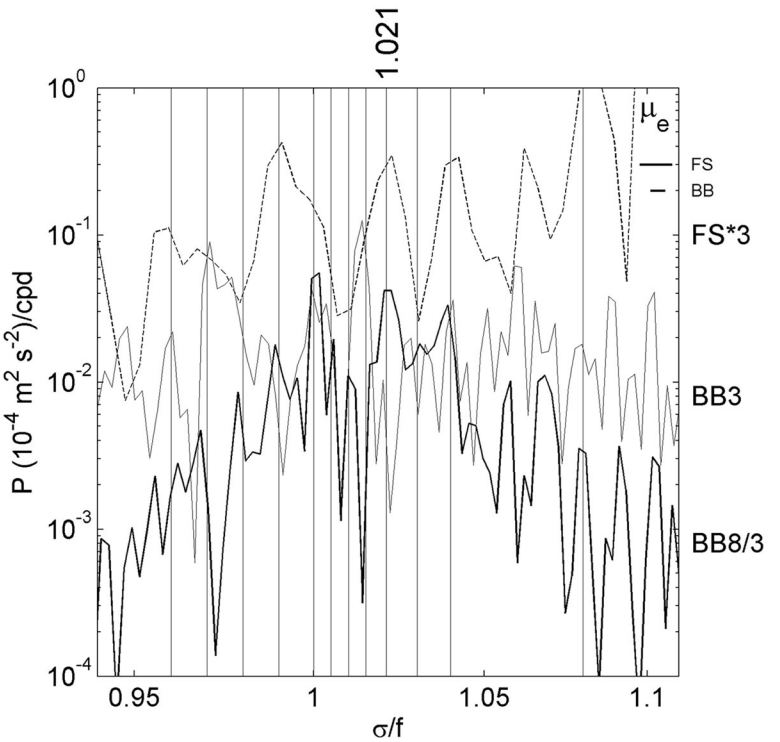

Figure 6. As Figure 4 but for the inertial band, scaled with local f to have all mooring sites in one graph.

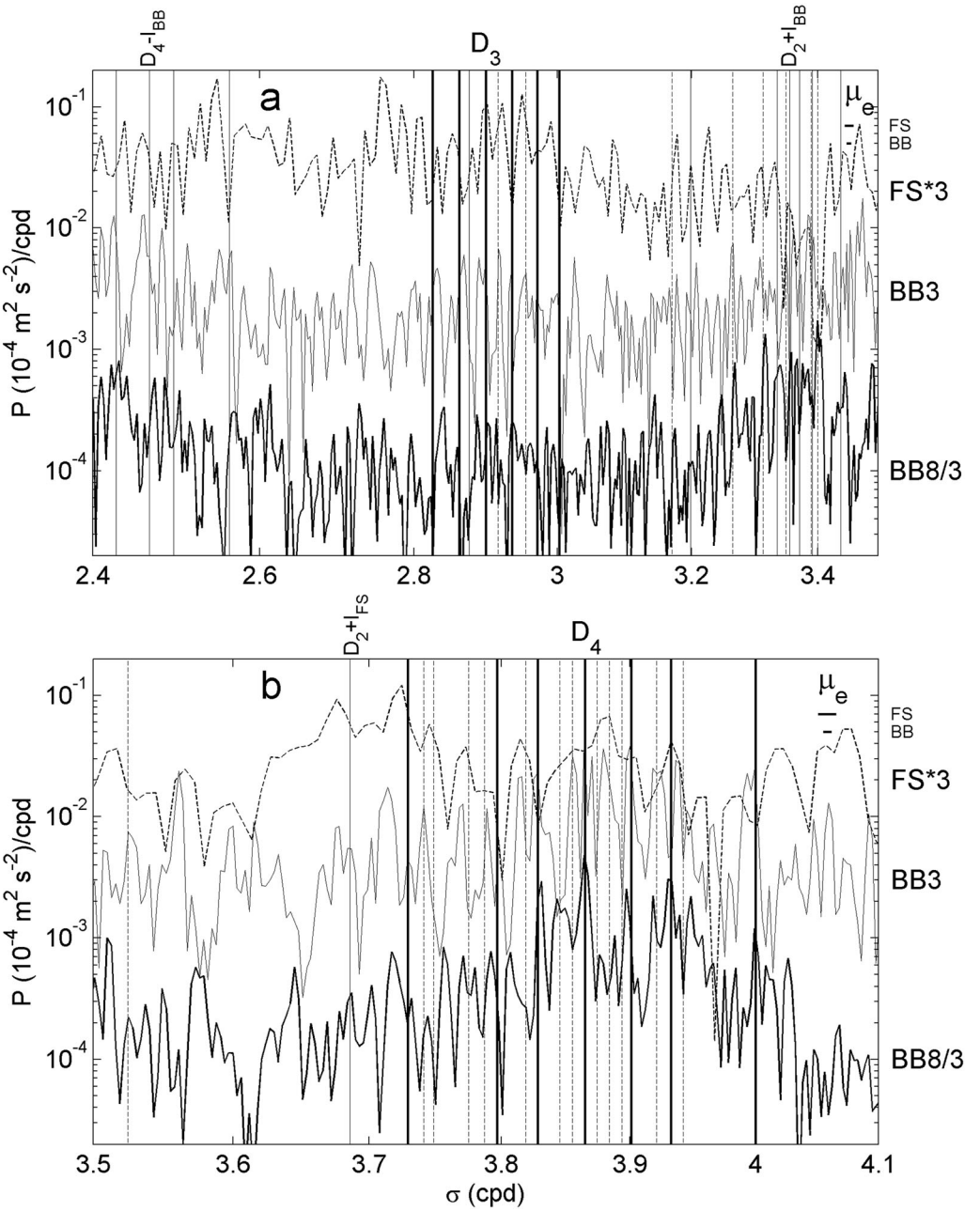

Figure 7. As Figure 4 but for $2.4 < \sigma < 4.1$ cpd. No [&]-frequencies are indicated. (a) Ter-diurnal (D_3) and semi-diurnal(D_2)-inertial(I; for BB) bands. Note that f(BB3) = f(BB8) + 0.0209 cpd. (b) quarter-diurnal band (D_4) including semi-diurnal(D_2)-inertial(I) band in FS.

split-M_1 at $(1.000 \pm 0.005)M_1$ is seen in the BB8 data. The latter suggests sub-harmonics predominantly of semidiurnal internal waves after interaction with sub-inertial motions, and no involvement of barotropic M_2.

Adopting a similar quasi-deterministic viewpoint as for tides, the near-inertial band ("I") also shows peaks that extend above the continuum at least like the incoherent baroclinic tidal motions (Figure 6). At BB8, peaks are observed at frequencies like f, (1.000 ± 0.005)f, 1.01f, 1.015f, 1.021f, 1.03f, 1.04f. The peak at 1.02 ± 0.006f is dominant in many BB-records. In the FS, also 0.99f is relatively energetic. As for the BB the frequency ratio $M_2/f \approx 1.35 \neq 1$, the same multiplication factor in the split of frequency lines for inertial and semi-diurnal constituents suggests nonlinear effects due to (similar) remote background effects, rather than just local interactions.

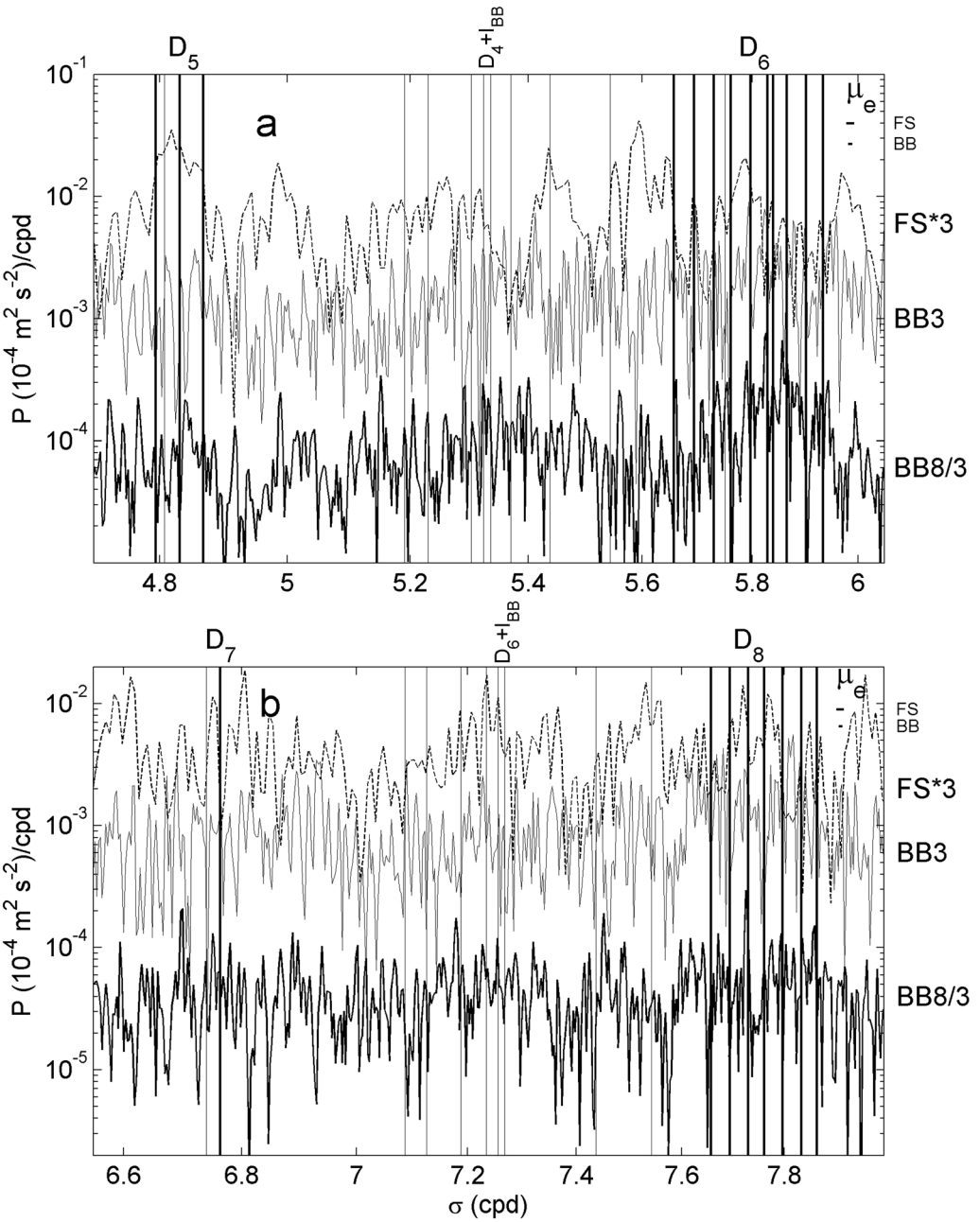

Figure 8. As Figure 4 but for $4.7 < \sigma < 8$ cpd. No $^{\&}$-frequencies are indicated. (a) Fifth-diurnal (D_5) and sixth-diurnal (D_6) bands, including quarter-diurnal-inertial (for BB) band. (b) seventh-diurnal (D_7) – eighth-diurnal (D_8) bands, including sixth-diurnal-inertial band (for BB).

However, local interactions seem important in filling the remainder of the spectrum. As higher tidal harmonics are entirely due to nonlinear interactions between principal tidal constituents, one expects motions at these frequencies to have a deterministic character too. Each band, for instance fourth-diurnal D_4, with respect to the continuum outside these bands is composed of many components due to different combinations between principal (semi-diurnal) constituents (Figures 7 and 8; Table 2). In Figures 7 and 8 only FS- and BB8-data are presented, for clarity. The list in Table 2 is not exhaustive, because not all higher tidal harmonics are observed (Figures 7 and 8). Essentially, like for the semi-diurnal band, only a few of the peaks in each band (e.g., D_4) are assigned to tidal constituents. All others are at non-tidal frequencies that are related to the tidal constituents through nonlinear interaction, either directly with the slowly varying background, or indirectly from tidal constituents modified by the same background at their principal frequencies. For example,

nonlinear motions resulting from interactions between motions at frequencies like $(1.000 \pm 0.005)M_2$ are found back in higher harmonic bands: $2(1.005M_2)$, $2(0.995M_2)$, $(1.000 + 1.005)M_2$, $1.000 + 0.995)M_2$, but also $M_4 + 0.01$ cpd $= 2(1.0025M_2)$. In the fourth-diurnal band these "non-tidal" constituents exceed in amplitude most known tidal (interaction) constituents. Like in Figures 4–6, the solid vertical lines in Figures 7 and 8 indicate tidal and inertial interaction constituents, of which all tidal components are shown as in RL. The dashed vertical lines indicate (a few of the) non-tidal constituent interaction frequencies that are recognized in the spectra, like the examples given above. Variations between the spectra are not only due to varying background conditions, but also due to varying (tidal) interactions. For example, even tidal harmonics are usually much more energetic than odd harmonics (e.g., ter-diurnal D_3), except in FS-data. As noted before, the main difference between FS- and BB-spectra is the level between tidal harmonic and tidal-inertial interaction bands, reflecting the much broader effects of interactions with a broader sub-inertial band in the FS-data.

Many more interactions exist, for instance also in frequency ranges well outside inertial-tidal interaction frequencies, such as 1.7, 2.4 cpd and at sub-inertial frequencies of which $|M_2 - S_2| = 0.068$ cpd, $|S_2 - N_2| = 0.104$ cpd and $|M_2 - N_2| = 0.036$ cpd are known, to which one can add $|1.005M_2 - S_2| = 0.058$ cpd and $|1.005M_2 - M_2| = 0.01$ cpd, etcetera.

5. Discussion and Conclusions

The inspection of the tidal bands D_1 and D_2 and the nonlinear tidal-tidal interaction bands in current meter spectra shows that these deterministic signals extend more or less out of the background continuum, just like in pressure (tide gauge) spectra. As near-inertial motions are the ocean adjustment to (atmospheric) disturbances, their quasi-deterministic initial response becomes modified by nonlinear interactions in much the same way as incoherent (internal) tidal motions [cf. *van Haren*, 2004b]. It is suggested that all these modified signals together construct the ocean "continuum" spectrum, following the GM-slope in the ocean interior and a steeper slope near internal tide sources [*van Haren et al*., 2002]. Because internal tidal and inertial motions are directly related to the main sources of ocean motions together with large-scale low-frequency motions, their higher harmonics extend above this ocean continuum. The continuum itself is attributable to tidal-inertial interactions, albeit to second order only after interaction with the sub-inertial motions. This result is independent of the taper window used (Figure 1), as such window removes all side bands by four or more decades, theoretically. As long as there is sufficient density stratification, many higher tidal harmonics are observed well above the instrumental noise levels. As a result, quasi-deterministic, non-stochastic signals determine the smoothly sloping spectral continuum and dominate the internal wave band of observed kinetic energy spectra, rather than incoherent signals as proposed for temperature spectra [*Radok et al*., 1967]. The quasi-random statistics commonly applied for "statistical significance" are thus less suited for well-moored Eulerian current meter data. Such data are better treated as deterministic signals, like tide gauge data.

Due to the non-stochastic character of moored current data, we can potentially learn more about climate variations from the ocean continuum, interpreting it and its cusps as the modulation of several (tidal-inertial) carriers as was contemplated by *Munk et al*. [1965]. This is because, any variations in background stratification will modify (internal wave) shear and therefore sub-inertial motions and the spectral level in the internal wave band (*cf*. Figures 2 and 3). Following the deep-sea observations here, the best means for investigating such variations from spectra are point measurements, because the nonlinear interaction between propagating tidal-inertial waves and sub-inertial motions occurring along an internal wave path result in different observations varying in time and space. Thus, spatial smoothing over typical internal wave scales O(100 m), like for example in ADCP data, averages some of the information of non-random incoherent motions and therefore information on the sub-inertial motions. This probably explains in part the clearer tidal spectra in FS data compared to RCM-8 BB data (Figures 4 and 5), in addition to the difference in sub-inertial motions.

We note that the investigated spectra present averages of 5 and 11 months of observations. The temporal variations in the sub-inertial motions passing each sensor certainly provide different ocean continuum spectra from year to year, but a certain level will always be detected. This partially explains the different spectral continua observed at the different sites (Figure 3), reflecting the different low-frequency current and stratification variations: across most of the spectrum ($\sigma \leq 8$ cpd) the BB-spectra scale with a constant factor, either

the mean background N or shear magnitude |**S**|, except at inertial and inertial-interaction frequencies [*van Haren*, 2004b]. The FS-spectrum shows the same levels at the tidal-inertial interaction frequencies as the BB3-spectrum, which is understood because of approximately the same level of tidal and sub-inertial energies. The much more filling of the gaps between the groups of interaction frequencies is attributed to the much broader sub-inertial part in the FS-spectrum, resulting in a more complete filling of the internal wave band following interactions. Qualitatively, the present observations suggest a nonlinear concept for N- (or |**S**|-) scaling of the internal wave spectrum, thereby also explaining the importance of tidal and inertial motions and the lack of gaps in the observed spectra.

To study internal wave climatology in a search for internal wave sources and modifications [*Wunsch*, 1975] we require better spectral resolution. As a result we need longer time series of current observations, for example as in the Ultramoor project [*Frye et al*., 2002]. A more precise and quantitative model describing the present observations is also welcomed. Does the continuum spectrum reflect self-organized criticality: tides generating rectified low-frequency, sub-inertial currents that generate background shear in balance with stratification that supports the internal waves, or should the focus be on the nonlinear tidal-tidal and tidal-inertial harmonics?

Acknowledgments
I enjoyed the assistance of the crew of the R/V Pelagia in the deployment and recovery of all moorings. The projects in the Bay of Biscay ("Triple B") and the Faeroe-Shetland Channel ("PROCS") were supported by grants from the Netherlands organization for the advancement of scientific research, NWO. Data use requests can be directed to hans.van.haren@nioz.nl.

References

Carter, G. S., and M. C. Gregg (2006), Persistent near-diurnal internal waves observed above a site of M_2 barotropic-to-baroclinic conversion, *J. Phys. Oceanogr.*, *36*, 1136–1147.
Emery, W. J., and R. E. Thomson (1998), *Data Analysis Methods in Physical Oceanography*, 634 pp., Pergamon, Amsterdam.
Frye, D., N. Hogg, and C. Wunsch (2002), New-generation mooring system allows longer deployment, *Eos Trans. AGU*, *83*(34), 365–371.
Garrett, C. J. R., and W. H. Munk (1972), Space-time scales of internal waves, *Geophys. Fluid Dyn.*, *3*, 225–264.
Jenkins, G. M., and D. G. Watts (1968), *Spectral Analysis and its Applications*, 525 pp., Holden-Day, San Francisco, Calif.
LeBlond, P. H., and L. A. Mysak (1978), *Waves in the Ocean*, 602 pp., Elsevier, Amsterdam.
Kim, Y. C., and E. J. Powers (1979), Digital bispectral analysis and its application to nonlinear wave interactions, *IEEE Trans. Plasma Sci.*, *7*, 120–131.
McComas, C. H., and M. G. Briscoe (1980), Bispectra of internal waves, *J. Fluid Mech.*, *97*, 205–213.
Munk, W., F. Snodgrass, and M. Wimbush (1970), Tides off-shore: transition from California coastal to deep-sea waters, *Geophys. Fluid Dyn.*, *1*, 161–235.
Munk, W. H., and D. E. Cartwright (1966), Tidal spectroscopy and prediction, *Philos. Trans. R. Soc. London A*, *259*, 533–581.
Munk, W. H., B. Zetler, and G. W. Groves (1965), Tidal cusps, *Geophys. J. R. Astron. Soc.*, *10*, 211–219.
Nuttall, A. H., and G. C. Carter (1980), A generalized framework for power spectral estimation, *IEEE Trans. Acoust. Speech Signal Process.*, *28*, 334–335.
Parks, T. W., and C. S. Burrus (1987), *Digital Filter Design*, 342 pp., John Wiley, N. Y.
Radok, R., W. Munk, and J. Isaacs (1967), A note on mid-ocean internal tides, *Deep Sea Res. Oceanogr. Abstr.*, *14*, 121–124.
Rossiter, J. W., and G. W. Lennon (1968), An intensive analysis of shallow water tides, *Geophys. J. R. Astron. Soc.*, *16*, 275–293.
van Haren, H. (2004a), Incoherent internal tidal currents in the deep-ocean, *Ocean Dyn.*, *54*, 66–76.
van Haren, H. (2004b), Bandwidth similarity at inertial and tidal frequencies in kinetic energy spectra from the Bay of Biscay, *Deep Sea Res., Part I*, *51*, 637–652.
van Haren, H., L. Maas, and H. van Aken (2002), On the nature of internal wave spectra near a continental slope, *Geophys. Res. Lett.*, *29*(12), 1615, doi:10.1029/2001GL014341.
Wunsch, C. (1975), Internal tides in the ocean, *Rev. Geophys.*, *13*, 167–182.